0273-2289/03/105-108/0867/$20.00

Continuous Clavulanic Acid Adsorption Process

Renata M. R. G. Almeida,* Marlei Barboza, and Carlos O. Hokka

Chemical Engineering Department, Federal University of Sao Carlos, Via Washington Luiz, Km 235, 13565-905, Sao Carlos, SP, Brazil, E-mail: prmrg@iris.ufscar.br

Abstract

Adsorption kinetics and equilibrium data of clavulanic acid, a β-lactam antibiotic, on ion-exchange resin Amberlite IRA 400 were utilized to carry out the modeling and simulation of a continuous adsorption process. These simulations allowed the estimation of yield, concentration, and purification factors of the process utilizing the product final concentration. Experimental runs of this process were carried out using the conditions pointed out by simulation studies. Comparison of the experimental results and those calculated by the proposed model showed that the model could describe very well the main features of the continuous process.

Index Entries: Clavulanic acid; continuous adsorption; purification process.

Introduction

The inhibitory activity of clavulanic acid (CA) against β-lactamases, enzymes that catalyze the β-lactam ring hydrolysis reaction, have been detected in cultures of the bacteria *Streptomyces clavuligerus*. The discovery of this β-lactam antibiotic was first reported in 1976 by Beecham *(1)*. Nowadays the combination of CA with amoxicillin is the most successful example of the use of a β-lactam antibiotic sensitive to β-lactamase together with an inhibitor of these enzymes.

Primary extraction of CA from the clarified broth can be done either by extraction from acidified broth into a water-immiscible organic solvent or by adsorption in an anion-exchange resin followed by elution from the resin with an aqueous salt solution *(2)*. However, this antibiotic has no strong hydrophobic groups and presents high degradation rates, which leads to low recovery yields during the purification process. This antibiotic

*Author to whom all correspondence and reprint requests should be addressed.

is highly unstable at a pH <5.0 and >7.0 and the degradation rate increases remarkably with the increase temperature *(3,4)*.

Continuous adsorption with adsorbent recycle appears to be an alternative process for purification of CA. The continuous process can reduce the mass transfer resistances that have to be dealt with in fixed-bed adsorption. This process can minimize product degradation by reducing the contact time required in batch operations with continuous withdrawal of the antibiotic. In addition, since it takes place in well-mixed tanks, temperature and pH gradients can be avoided, and, consequently, degradation is much lower than in conventional columns. Futhermore, the continuous process reduces the expenses with adsorbent because lesser amount of the resin is needed *(5)*.

Several investigators have studies similar continuous adsorption processes dealing with separation of proteins, enzymes *(5–7)*, and antibiotics *(8)*. Barboza et al. *(8)* proposed a mathematical model describing a continuous adsorption process for purification of cephalosporin C on a hydrophobic resin.

In the present work, adsorption kinetics and equilibrium data of CA on the ion-exchange resin Amberlite IRA 400 in the chloride cycle were utilized to carry out the modeling and simulation of a continuous adsorption process. The yield, concentration, and purification factors of the process were estimated utilizing the product final concentration obtained by simulations. Experimental runs of the continuous adsorption process were carried out using the simulation conditions, and the experimental results were compared with those calculated by the proposed model.

Materials and Methods

Adsorbate

CA was obtained from fermentation broth produced by *S. clavuligerus* ATCC 27064. Before the adsorption process, the fermentation broth was pretreated as follows: The broth was centrifuged to obtain a clear solution free of cells. Then the solution pH was brought down (3.5–4.0) to precipitate the soluble solids and proteins. Finally, the solution containing the product was centrifuged again and filtered through analytical paper filters to eliminate suspended impurities.

Preparation of Adsorbent

The stationary phase was the anion-exchanger Amberlite IRA 400, kindly supplied by Rohm and Haas. The resin was pretreated with 10% (w/v) NaCl and then washed several times with deionized water to eliminate the excess ions. NaCl (2%) was used as the eluent throughout.

Apparatus and Process Start-up

The adsorption reactors were stirred mechanically and considered to be perfectly mixed tank reactors. The process start-up was carried out by switching the pumps on. The reactor feed started with CA solution in the

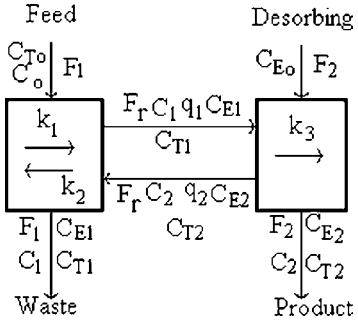

Fig. 1. Schematic flow sheet of the continuous processes for CA purification.

first stage and 2% NaCl in the second. The temperature in the first reactor was controlled at 10°C and in the second stage at 30°C. The outflowing solutions of each reactor were independent during the runs. The concentrations of CA with time were obtained by analyzing the samples in the exit stream of each stage.

Analytical Methods

The clavulanic acid concentrations were determined by high-performance liquid chromatography (HPLC), as described by Foulstone and Reading *(9)* by reaction with imidazole solution, pH 6.8. The HPLC equipment was operated at 28°C, with a flow rate of 2.5 mL/min. The mobile phase was composed of a 0.1 *M* KH_2PO_4 buffer solution containing 6% of methanol and phosphoric acid, which brings the pH to 3.2. Contaminants (CT) concentration were determined by spectrophotometer at 280 nm.

Mathematical Modelling

The basic principles of the theoretical model, previously described by Rodrigues et al. *(7)* for enzyme purification, were used. In the present work, the model incorporates external liquid film mass transfer coefficient, pore diffusion, and kinetic equations for adsorption and desorption in each stage. It also accounts for the presence of inert contaminants in the CA feed stream. These contaminants can be considered as usual fermentation broth components such as sugars, pigments, amino acids, and proteins in solution.

The mathematical model of the process was obtained essentially by accomplishing a mass balance in each reactor including the adsorption/desorption equations. A schematic view of this process is illustrated in Fig. 1. The process operates as follows: The sample is fed continuously to the first reactor, the adsorbing stage, where it contacts the ionic adsorbent beads and is adsorbed. The beads, with the adsorbed product, are then pumped to the desorbing stage in the second reactor, where the addition of the eluent (NaCl solution) causes the desorption of the antibiotic. The spent beads are then recycled to the adsorption stage, while the antibiotic is removed. Both reactors are well agitated.

To reduce the number of variables, four global variables were previously defined, as shown by Eqs. 1–4, for reactor residence time (θr_1 and θr_2) and solids residence time (θs_1 and θs_2).

$$\theta r_1 = \frac{V_1}{F_1 + F_r \varepsilon_{r1}} \tag{1}$$

$$\theta r_2 = \frac{V_2}{F_2 + F_r \varepsilon_{r2}} \tag{2}$$

$$\theta s_1 = \frac{V_1}{F_r \varepsilon_{r1}} \tag{3}$$

$$\theta s_2 = \frac{V_2}{F_r \varepsilon_{r2}} \tag{4}$$

The reactor residence time is the ratio between the liquid total volume and the global liquid feeding rate. The solids residence time is the ratio of the amount of resin in the reactor by the out flow rate of the resin from the reactor. The values of the flow rates (F_1, F_2, and F_r), as they are presented, are calculated based on the established reactor residence times and solids residence times, as described by Eqs. 1–4.

The differential equations representing the system behavior, in both stages, are described next.

First Stage

CA BALANCE

INTRAPARTICLE DIFFUSION

$$\varepsilon_p \frac{\partial C_{i1}}{\partial t} = D_{efk} \varepsilon_p \left(\frac{\partial^2 C_{i1}}{\partial r^2} + \frac{2}{r} \frac{\partial C_{i1}}{\partial r} \right) - \left(1 - \varepsilon_p\right) \frac{\partial q_{i1}}{\partial t} \tag{5}$$

$$\frac{dq_{i1}}{dt} = k_1 C_{i1} (qm_1 - q_{i1}) - k_2 q_{i1} \tag{6}$$

The initial conditions are

$$t = 0 \rightarrow q_{i1} = C_{i1} = 0 \tag{7}$$

The boundary condition satisfying symmetry condition is

$$r = 0 \rightarrow \frac{\partial C_{ir}}{\partial r} = 0 \tag{8}$$

The boundary condition at the surface of the resin is

$$r = R \rightarrow \frac{\partial C_{i1}}{\partial r} = \frac{k_{s1}}{\varepsilon_p D_{efk}} \left(C_1 - C_{s1} \right) \tag{9}$$

LIQUID PHASE

$$\frac{\partial C_1}{dt} = \frac{\left(C_0 - C_1\right)\left(\theta s_1 - \theta r_1\right)}{\left(\theta s_1 \theta r_1\right)} + \frac{1}{\theta s_1}\left(C_2 - C_1\right) + \left(-k_1 \overline{C}_1\left[qm_1 - \bar{q}_1\right] + k_2 \bar{q}_1\right)\frac{\left(1-\varepsilon_r\right)}{\varepsilon_r} \quad (10)$$

SOLID PHASE

$$\frac{d\bar{q}_1}{dt} = \frac{1}{\theta s_1}\left(\bar{q}_2 - \bar{q}_1\right) - \left(-k_1 \overline{C}_1\left[qm_1 - \bar{q}_1\right] + k_2 \bar{q}_1\right) \quad (11)$$

Here, $\bar{q}_1$ and $\overline{C}_1$ are the mean value calculated by the weights of the Radau quadrature (Eqs. 12 and 13) with contour in the surface of the solid or Gaussian quadrature (Eq. 14) when some contour is not considered in the surface *(10)*.

$$\bar{q}_1 = w_0 \cdot q_{j(r=1)} + \sum_{j=1}^{N} q_j w_j \quad (12)$$

$$\overline{C}_1 = w_0 \cdot C_{j(r=1)} + \sum_{j=1}^{N} C_j w_j \quad (13)$$

$$\bar{q}_1 = \sum_{j=1}^{N} q_j w_j \quad (14)$$

in which N is the number of collocation points and w_j are the weights of the Radau quadrature (Eqs. 12 and 13) or Gauss (Eq. 14).

$\overline{C}_1$ can be easily calculated using the principle of the Eq. 13. In the present study, $\bar{q}_1$ and $\bar{q}_2$ were obtained by Eq. 14.

ELUENT BALANCE

$$\frac{dC_{E1}}{dt} = \frac{-C_{E1}\left(\theta s_1 - \theta r_1\right)}{\left(\theta s_1 \theta r_1\right)} + \frac{1}{\theta s_1}\left(C_{E2} - C_{E1}\right) \quad (15)$$

INERT CONTAMINANTS BALANCE

$$\frac{dC_{T1}}{dt} = \frac{\left(C_{T0} - C_{T1}\right)\left(\theta s_1 - \theta r_1\right)}{\theta s_1 \theta r_1} + \frac{1}{\theta s_1}\left(C_{T2} - C_{T1}\right) \quad (16)$$

Second Stage

CA BALANCE

INTRAPARTICLE DIFFUSION

$$\varepsilon_p \frac{\partial C_{i2}}{\partial t} = D_{ef2}\varepsilon_p\left(\frac{\partial^2 C_{i2}}{\partial r^2} + \frac{2}{r}\frac{\partial C_{i2}}{\partial r}\right) - \left(1-\varepsilon_p\right)\frac{\partial q_{i2}}{\partial t} \quad (17)$$

$$\frac{dq_{i2}}{dt} = -k_3 q_{i2} \tag{18}$$

The initial conditions are

$$t = 0 \rightarrow q_{i2} = C_{i2} = 0 \tag{19}$$

The boundary condition satisfying the symmetry conditions is

$$r = 0 \rightarrow \frac{\partial C_{i2}}{\partial r} = 0 \tag{20}$$

The boundary condition at the surface is

$$r = R \rightarrow \frac{\partial C_{i2}}{\partial r} = \frac{k_{s2}}{\varepsilon_p D_{ef2}} \left(C_2 - C_{s2}\right) \tag{21}$$

LIQUID PHASE

$$\frac{dC_2}{dt} = \frac{-C_2\left(\theta s_2 - \theta r_2\right)}{\theta s_2 \theta r_2} + \frac{1}{\theta s_2}\left(C_1 - C_2\right) + \left(k_3 \overline{q}_2\right)\frac{\left(1-\varepsilon_r\right)}{\varepsilon_r} \tag{22}$$

SOLID PHASE

$$\frac{d\overline{q}_2}{dt} = \frac{1}{\theta s_2}\left(\overline{q}_1 - \overline{q}_2\right) - k_3 \overline{q}_2 \tag{23}$$

Here, $\overline{q}_2$ is calculated in the same manner as in the first stage.

ELUENT BALANCE

$$\frac{dC_{E2}}{dt} = \frac{\left(C_{E0} - C_{E2}\right)\left(\theta s_2 - \theta r_2\right)}{\left(\theta s_2 \theta r_2\right)} + \frac{1}{\theta s_2}\left(C_{E1} - C_{E2}\right) \tag{24}$$

INERT CONTAMINANTS BALANCE

$$\frac{dC_{T2}}{dt} = \frac{C_{T2}\left(\theta s_2 - \theta r_2\right)}{\left(\theta s_2 \theta r_2\right)} + \frac{1}{\theta s_2}\left(C_{T1} - C_{T2}\right) \tag{25}$$

The model is represented by a set of partial differential equations (Eqs. 5 and 17), and they were reduced to a set of ordinary differential equations by the method of orthogonal collocation. Two internal collocation points with two additional collocation points corresponding to the two boundary conditions were used. The set of ordinary differential equations was solved by the Runge Kutta method of fourth order.

Equations 15, 16, 24, and 25 were formulated by assuming that no adsorption of eluent and contaminants occurs. The differential equations can be solved in the steady state, and C_1 and C_2 can be evaluated for defined operational conditions, which facilitates the process performance

Table 1
Simulation Parameters

Run	C_0 (g/L)	θr_1 (min)	θr_2 (min)	θs_1 (min)	θs_2 (min)	ε_{r1} (–)	ε_{r2} (–)	V_1 (mL)	V_2 (mL)
1	0.100	71.3	44.1	108.0	154.8	0.86	0.60	130	130
2	0.100	71.3	44.1	108.0	107.2	0.86	0.60	130	90
3	0.100	81.0	30.6	101.1	100.7	0.86	0.60	130	90
4	0.100	81.0	30.6	101.1	65.2	0.86	0.60	200	90

Table 2
Operation Conditions

Run	F_1 (mL/min)	F_2 (mL/min)	F_r (mL/min)
1	0.62	2.10	1.39
2	0.62	1.20	1.39
3	0.32	2.04	1.49
4	0.49	1.56	2.30

analysis in terms of important parameters such as the performance parameters yield (Y), concentration factor (CF), and purification factor (PF), defined by Eqs. 26, 27, and 28, respectively:

$$Y = 100 \frac{C_2 F_2}{C_0 F_1} \tag{26}$$

$$CF = \frac{C_2}{C_0} \tag{27}$$

$$PF = \frac{C_2 \cdot C_{T0}}{C_0 \cdot C_{T2}} \tag{28}$$

Y is the ratio between the mass of the desired product recovered and the mass of the same product fed into the system. CF is the ratio between product concentration in the product stream and the product concentration in the feed stream (Fig. 1). PF is the ratio between CF of the desired product (C_2/C_0) and CF of the contaminants (C_{T2}/C_{T0}).

Results and Discussion

The continuous adsorption process of CA was simulated to obtain information about its dynamic behavior. The values of liquid phase ratio, initial concentration of CA, reactor residence time, solids residence time, and reactor volume used in the simulation runs are presented in Table 1. These parameters were settled based on the flow rates and volumes of a similar process described by Barboza et al. *(8)*.

The flow rates regarding each run are given in Table 2; they were calculated utilizing Eqs. 1–4 and the values of Table 1.

Table 3
Transport and Kinetic Parameters

	D_{ef} (cm^2/s)	k_s (cm/s)	k_1 (L/[g·min])	k_2 (min^{-1})	k_3 (min^{-1})
Adsorption	9.0×10^{-5}	5.30×10^{-2}	1.70	0.13	—
Desorption	9.0×10^{-5}	7.65×10^{-2}	—	—	9.5×10^{-2}

Table 4
Equilibrium Parameters

Parameter	T (°C)	pH	q_m (g_{CA}/g_{res})	K_D (g/L)
Isotherm	10	6.2	1.14×10^{-2}	7.90×10^{-2}

Transport and kinetic parameters (D_{ef}, k_s, k_1, k_2, and k_3) were determined by simulations of kinetic studies in batch runs for both adsorption and desorption stages. These parameters are given in Table 3. Equilibrium parameters of the Langmuir model are presented in Table 4. With the data of Tables 1, 3, and 4 the continuous adsorption process of CA on resin Amberlite IRA 400 was simulated.

Figures 2A–D shows the CA and contaminants concentration profiles in the exit stream from each stage for runs 1–4, respectively. CA was adsorbed on the resin Amberlite IRA 400 in the first reactor and was desorbed by NaCl solution in the second one. Contaminants were present in both stages and this fact may result in a low purification factor. Figure 2 shows that CF in all runs was very low because CA concentration at the desorption stage was lower than at the adsorption stage. The process equilibrium time was 5 h.

The performance parameters Y, PF, and CF were determined for all runs and are presented in Table 5. This proposed process was able to furnish a high yield but it was not able to give a concentrated product, as shown by the low values of CF at all runs. It was observed that CA concentration in the exit of the second stage was higher than contaminants concentration, giving a PF >1. Recently, Mayer et al. *(11)* reported values of Y of about 60%, CF of about 2.0, and PF of approx 1.4 in a CA recovery process in fixed-bed columns on the same adsorbent. Good CF values were found, but PF values were in the same range and the Y values were quite low compared with the results presented in Table 5.

Comparison of the yields of runs 4 (V_1 = 200 mL) and 3 (V_1 = 130 mL) in Table 5 reveals that the highest yield was obtained utilizing a higher volume at the first reactor. The same reactor residence time and solid residence time were used at both runs, but at run 4 the yield was 12% higher than at run 3. For the second reactor, it was better to utilize a smaller volume, as shown by comparing runs 1 (V_2 = 130 mL) and 2 (V_2 = 90 mL).

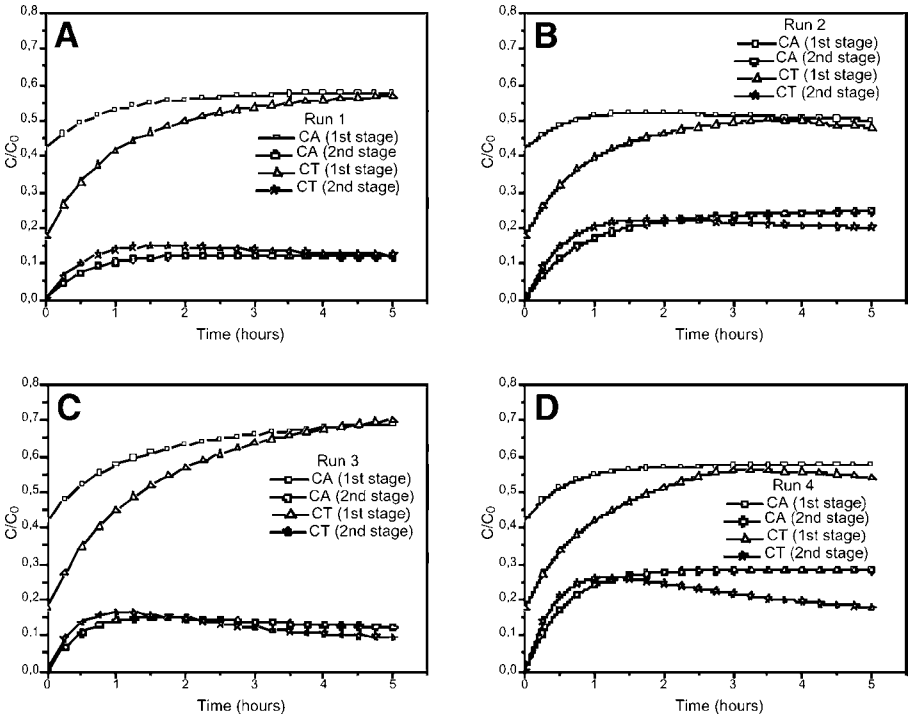

Fig. 2. Simulations of CA adsorption continuous process: **(A)** run 1; **(B)** run 2; **(C)** run 3; **(D)** run 4.

Table 5
Simulated Results of Y, PF, and CF

Run	Y (%)	PF (–)	CF (–)
1	41.1	0.95	0.12
2	48.0	1.23	0.25
3	79.0	1.29	0.12
4	90.0	1.57	0.28

The best results of Y, PF, and CF were obtained at run 4, but it is not possible to say that run 4 had the optimum parameters because the process used is multivariable. Optimum conditions can be obtained utilizing optimization techniques included in the model. However, the optimization techniques can lead to constrained optimum values of Y, CF, and PF, requiring further pilot-plant and economical studies for a definite conclusion.

Experimental runs were carried out using the operation conditions of the simulated runs 2 and 4 (Table 2) in order to validate the model. The conditions of runs 2 and 4 are presented in Figs. 3 and 4, respectively.

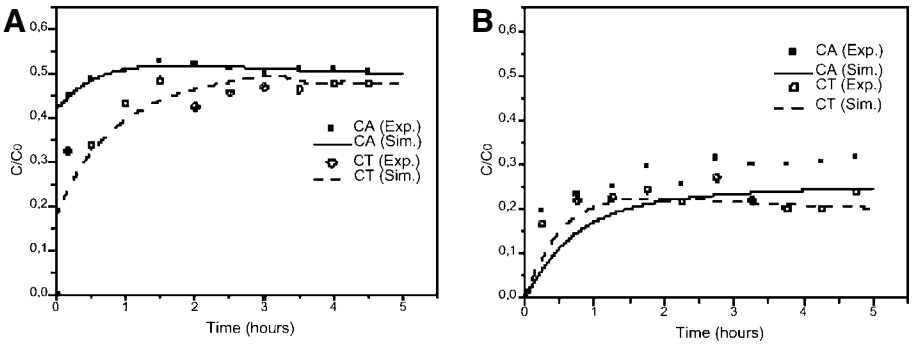

Fig. 3. Simulated and experimental results of CA adsorption continuous process of run 2: **(A)** first reactor; **(B)** second reactor.

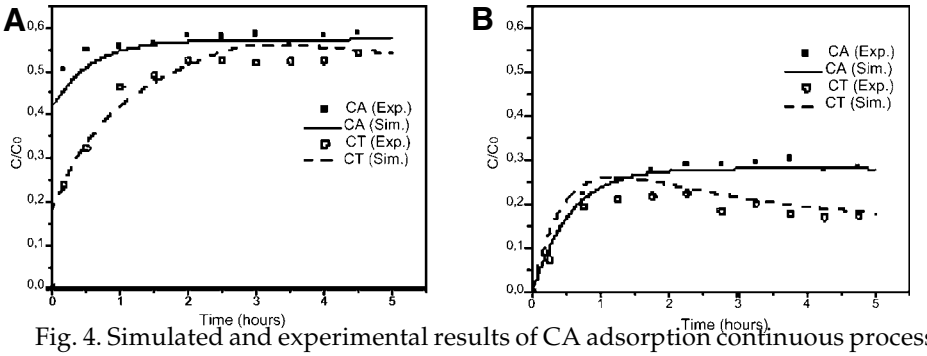

Fig. 4. Simulated and experimental results of CA adsorption continuous process of run 4: **(A)** first reactor; **(B)** second reactor.

Figure 4 shows that the fits of CA and CT in both stages were good, but Fig. 3 it shows that the model fitted CA data well in the adsorption reactor but not in the desorption one. Since the volume of the first reactor in run 2 was lower than in run 4, it was expected that in run 2 a lower concentration than in run 4 in the desorption step would be achieved, around 0.25, like simulation. However, the concentration was equal to run 4 and, consequently, higher than obtained in the simulation. Further experiments, in different conditions, will be necessary to elucidate this behavior. Figures 3 and 4 also shown that CA concentration in the second reactor was lower than in the first, so, like the model predicted, a low CF was also obtained in the experimental runs.

The parameters Y, PF, and CF were calculated for experimental runs and are shown in Table 6, together with the parameters obtained by simulation and the difference between the experimental and the simulated results. The data in Table 6 show that the model predicted the performance parameters with the differences between experimental and simulated data lower than 17%. These differences can be related to some operational prob-

Table 6
Simulated and Experimental Results of Y, PF, and CF
and Difference Between Experimental and Simulated Results (*e*)

	Y (%)			PF (–)			CF (–)		
Run	Exp.	Sim.	*e* (%)	Exp.	Sim.	*e* (%)	Exp.	Sim.	*e* (%)
2	58.10	48.00	17	1.48	1.23	17	0.30	0.25	17
4	96.90	90.00	7	1.69	1.57	7	0.31	0.28	9

[a] Exp., experimental; Sim., simulated.

lems in the experimental runs. For instance, a severe practical limitation of this continuous process, as proposed here, is the recirculation of adsorbent beads between the two reactors. This recirculation was sometimes manually operated because the beads frequently obstructed the pump. However, a steady flow could be attained most of the time.

The overall purpose of the model was to predict the general behavior of the system and this purpose was attained. The model can be used to determined the process parameters such as Y, PF, and CF obtained in several different conditions and therefore can be used as a tool for optimization of the multivariable process and process control and design. As an example, the model can be used to optimize the process in order to improve Y, CF, and PF, up to a level allowing economical operation of an industrial plant.

From an industrial point of view, the continuous adsorption process is feasible for use in combination with fermentation utilizing a filtration system to remove cells and proteins in the fermentation broth. The size of both fermentation and purification vessels should be established in such a way that the fermentation step (batch) proceeds directly to a continuous operation of the purification step.

Conclusion

Based on the CF, PF, and Y, the process performance was evaluated. The experimental and simulated data of these parameters were compared, and the differences between them were, in most cases, lower than 17%. This fact shows the good agreement of the model with the experimental data.

A model of a continuous process for CA separation was described, incorporating a kinetic model. This validated model, together with key experimental data, can be a powerful tool to optimize and scale up this purification process.

Nomenclature

C_k = CA concentration in the solution (g/L)
C_{ik} = CA concentration inside the particles (g/L)

C_{Sk} = CA concentration at particle surface (g/L)
C_{Ek} = NaCl concentration (%)
C_{Tk} = contaminant concentration (g/L)
D_{efk} = effective diffusivity of CA (cm^2/s)
e = difference between simulated and experimental data (%)
F_k = flow rate of feeding (mL/min)
F_r = flow rate of recycle (mL/min)
K_D = Langmuir equilibrium constant (g/L)
K_{Sk} = mass transfer coefficient (cm/s)
k_1 = intrinsic kinetic constant for adsorption stage (g/[L·min])
k_2 = intrinsic kinetic constant for adsorption stage (min^{-1})
k_3 = intrinsic kinetic constant for desorption stage (min^{-1})
N = number of points of collocation (–)
q_{mk} = kinetic equilibrium parameter (g_{CA}/g_{res})
q_k = average amount of CA adsorbed in each stage (g_{CA}/g_{res})
q_{ik} = amount adsorbed in present particle along position r (g_{CA}/g_{res})
V_k = volume of present liquid phase (m/L)
w_j = weights of Radau quadrature (Eqs. 13 and 14) or Gauss (Eq. 12)
ε_{rk} = volume phase ratio, liquid to total phase volume (–)
ε_p = porosity of resin (–)
θ_{rk} = reactor residence time (min)
θ_{sk} = solid residence time (min)

Subscripts

k = 0 = initial
k = 1 = first stage
k = 2 = second stage

Acknowledgment

We wish to acknowledge Fundação de Amparo à Pesquisa do Estado de São Paulo (Process No. 99/07693-2, 99/03279-7, and 98/11596-0) for financial support.

References

1. Brown, A. G., Butterworth, D., Cole, M., Hanscomb, G., Hood, J. D., Reading, C., and Rolinson, G. N. (1976), *J. Antibiot.* **29,** 668–669.
2. Butterworth, D. (1984), in *Biotechnology of Industrial Antibiotics*, vol. 6, Vandamme, E. J., ed., Marcel Dekker, New York, NY, pp. 225–235.
3. Haginaka, J., Nakagawa, T., and Uno, T. (1981), *Chem. Pharm. Bull.* **29,** 3334–3341.
4. Mayer, A. F., Hartmann, R., and Deckwer, W. D. (1997), *Chem. Eng. Sci.* **52,** 4561–4568.
5. Pungor, E., Afeyan, N. B., Gordon, N. F., and Cooney, C. L. (1987), *Bio/Technology* **5,** 604–609.
6. Afeyan, N. B., Gordon, N. F., and Cooney, C. L. (1989), *J. Chromatogr.* **47,** 1–19.
7. Rodrigues, M. I., Zaror, C. A., Maugeri, F., and Asenjo, J. A, (1992), *Chem. Eng. Sci.* **47(1),** 263–269.
8. Barboza, M., Hokka, C. O., and Maugeri, F. (2002), *Bioprocess Biosystem Eng.* **25,** 193–203.
9. Foulstone, M. and Reading, C. (1982), *Antimicrob. Agents Chemother.* **22,** 753–762.

10. Villadsen, J. and Michelsen, M. L. (1978), *Solution of Differential Equation Models by Polynomial Approximations*, Prentice Hall, Englewood Cliffs, NJ.
11. Mayer, A. F., Anspach, F. B., and Deckwer, W. D. (1996), *Bioseparation* **6,** 25–39.